Dalton Transactions

ROYAL SOCIETY OF CHEMISTRY

PAPER

View Article Online
View Journal | View Issue

Check for updates

Cite this: *Dalton Trans.*, 2024, **53**, 7751

Hexadentate poly-Lewis acids based on the bowl-shaped tribenzotriquinacene†‡

Maurice Franke, Maximilian J. Klingsiek, Julian Buth, Jan-Hendrik Lamm, Beate Neumann, Hans-Georg Stammler and Norbert W. Mitzel *

Received 7th February 2024,
Accepted 20th February 2024

DOI: 10.1039/d4dt00379a

rsc.li/dalton

Hexadentate poly-Lewis acids (PLA) based on the bowl-shaped tribenzotriquinacene (TBTQ) have been synthesised. The introduction of three *n*-propyl groups into the benzhydrylic positions of the TBTQ backbone has significantly increased the solubility of the subsequently derived compounds. Semi-flexible PLAs containing boron and aluminium were obtained by hydrometallation of the corresponding 2,3,6,7,10,11-hexaalkynyl-TBTQ. Other rigid hexadentate PLAs were synthesised by stannylation of the corresponding alkyne units with Me_3SnNMe_2 followed by tin-element exchange reactions. The Lewis acidity of these PLAs was investigated in host–guest experiments with pyridine. Further experiments with bidentate bases showed correlations between their flexibility, their Lewis basicity and the complexation behaviour towards the synthesised PLAs. Addition of bis((dimethylphosphino)methyl)dimethylsilane (BisPhos) to solutions of the rigid alkynyl PLAs led to the formation of 3 : 1 adducts. Single crystal X-ray diffraction was used to further elucidate the host–guest connectivity. In addition, a sixfold pnictogen-bonding donor was synthesised by tin-antimony exchange.

Introduction

Unlike the well-known poly-Lewis bases, such as crown ethers and cryptands,[1] which have multiple Lewis basic sites, poly-Lewis acids (PLAs) feature several Lewis acid functions attached to an organic backbone. In addition to the commonly used Lewis acid functions based on elements such as mercury,[2] silicon,[3] and tin,[4] elements of the third main group including boron,[5] aluminium,[6] gallium[7] and indium[6d,8] are also often used. Of course, there are also examples of PLAs with elements of the fifth group, such as the bidentate antimony-based system developed by Gabbaï *et al.*[9] The synthesis of the Lewis acids is typically carried out by salt elimination, exchange reactions or hydrometallations. In addition to their applications in anion sensing[3b,5a,b,10] and catalysis,[5g,11] the complexation of small molecules in host–guest experiments,[7d,12] is the subject of current research. While early examples of PLAs were often based on small organic backbones such as alkyl[5b,6d] or phenyl derivatives,[7a,13] there is now a wide range of examples based on larger backbones, including derivatives of naphthalene,[5a,14] anthracene[5c,d,6d,9b] and even cyclic molecules.[3c,4c,6f,7b,c] A fascinating example of an organic backbone is the bowl-shaped tribenzotriquinacene (TBTQ) of C_{3v} symmetry. TBTQ was first synthesised in 1984 by Kuck *et al.*[15] It offers the unique advantage of being able to undergo three substitutions at the benzhydrylic positions, as well as six substitutions at the peripheral aromatic positions (Scheme 1).[16] An updated and efficient synthetic protocol introduced by Hopf *et al.*[17] in 2012 has further increased the versatility of TBTQ derivatives, making them valuable building blocks in the field of supramolecular chemistry. There are examples of TBTQ units linked to nanotubes,[18] cubes[19] and examples of cage-like TBTQ derivatives containing fullerenes.[20] Recently, we reported the synthesis of the first poly-Lewis acids based on the TBTQ backbone and the functionalisation with alkynyl spacers to obtain a TBTQ derivative bearing six tin

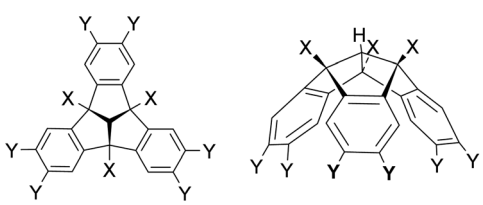

Scheme 1 Substitution pattern of the bowl-shaped tribenzotriquinacene (TBTQ) at the benzhydrylic (X) and the peripheral aromatic positions (Y).

Universität Bielefeld, Fakultät für Chemie, Lehrstuhl für Anorganische Chemie und Strukturchemie (ACS), Centre for Molecular Materials (CM2), Universitätsstr. 25, D-33615 Bielefeld, Germany. E-mail: mitzel@uni-bielefeld.de; https://www.uni-bielefeld.de/fakultaeten/chemie/ag/ac3-mitzel/

†Electronic supplementary information (ESI) available: ^{1}H, ^{11}B, ^{13}C, ^{19}F, ^{29}Si, ^{31}P, ^{119}Sn NMR spectra, crystallographic details. CCDC 2325781–2325787. For ESI and crystallographic data in CIF or other electronic format see DOI: https://doi.org/10.1039/d4dt00379a

‡Dedicated to Professor Dietmar Kuck on the occasion of his 75th birthday.

atoms.[21] However, the challenge we face is the poor solubility of these TBTQ derivatives when functionalised with six Lewis acid groups. This hinders further conversion into numerous poly-Lewis acids and subsequent study in host–guest experiments. To overcome this problem, we present a method to generate TBTQ derivatives with improved solubility, followed by synthesis of new PLAs based on the TBTQ backbone. These are thoroughly investigated in host–guest experiments to further our understanding of their applications in the field of poly-Lewis acids.

Results and discussion

Syntheses and characterisation of the hexadentate TBTQ derivatives

The triple hydrogenation of the allyl groups was carried out under conditions similar to those described by Kuck *et al.*[22] for a comparable TBTQ derivative at ambient temperature and pressure. Palladium on charcoal was used as a catalyst to afford the tri-*n*-propyl-TBTQ **2** in 93% yield. Sixfold bromination of compound **2** with iron powder and iodine as catalysts afforded the hexabromo-TBTQ **3** in 97% yield. A Sonogashira–Hagihara cross-coupling reaction of **3** with TMS-acetylene under CuI and $Cl_2[Pd(PPh_3)_2]$ catalysis introduced six trimethylsilyl-ethynyl-functions followed by cleavage of the $SiMe_3$ protecting groups by treatment with potassium fluoride in a THF/DMF solvent mixture similar to the conditions previously described by our group to give the hexaethynyl compound **5** (Scheme 2).[21]

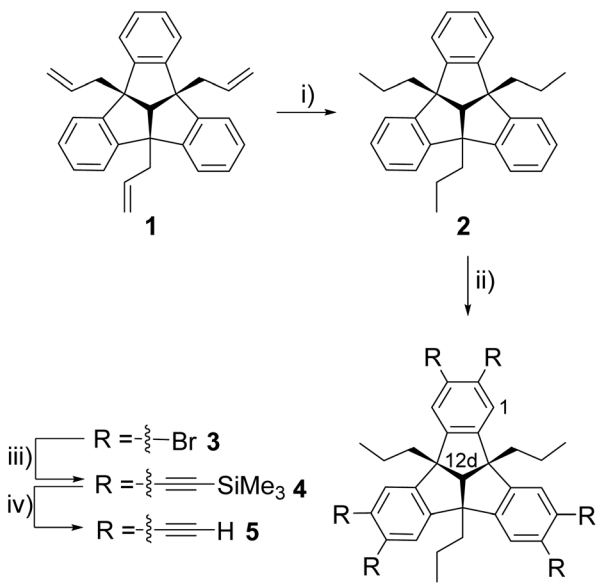

Scheme 2 Synthesis of 2,3,6,7,10,11-hexakis(ethynyl)-4b,8b,12b-tri-*n*-propyltribenzotriquinacene (**5**) starting from triallyl-TBTQ **1**. Reagents and conditions: (i) H_2, Pd/C, MeOH, rt, 3 d, workup, 93%. (ii) Br_2, I_2, Fe, $CHCl_3$, 60 °C, 16 h, workup, 97%. (iii) TMS-acetylene, $Cl_2[Pd(PPh_3)_2]$, CuI, PPh_3, Et_3N, 120 °C, 3 d, workup, 68%. (iv) KF, THF, DMF, rt, 4 d, workup, 40%.

Compounds **2–5** have been characterised by multinuclear NMR spectroscopy and elemental analysis. The ^{1}H NMR spectrum of **2** shows the characteristic signals for the hydrogen atoms at the peripheral benzene rings. By further functionalisation the ^{1}H NMR spectra of **3–5** show only a singlet for the remaining two hydrogen atoms on the outer sphere. Concerning the NMR spectra, all shifts agree well with the expectations, and the differences are only marginal (Table 1). In contrast to the elemental analyses of **2–4**, which fit well with the calculated values, we found that the carbon content of **5** was 3% too low (calcd: 93.78% measured: 90.99%), as reported for analogous compounds in previous work.[21] The NMR spectra give no indication of significant impurities. In contrast to the analogues with methyl substituents in the benzhydrylic positions,[21] the *n*-propyl-substituted compounds **2–5** are highly soluble in most common solvents.

Single crystals of **2–4** were obtained by slow evaporation of concentrated solutions in *n*-hexane and toluene, respectively, and analysed by X-ray diffraction experiments. The molecular structure of **4** is shown in Fig. 1 as an example.

Fig. 1 shows the orientation of the rigid alkyne units and the bowl shape of the TBTQ backbone. The bond lengths and angles are within the expected range and are comparable to the literature data of similar TBTQ compounds and the data of the molecular structures of **2** and **3**, respectively (see ESI† for details).

Hydrometallation reactions

Hexaethynyl-substituted TBTQ **5** was reacted with Piers' borane[23] in toluene solution, to give the hexadentate boron PLA **6** in quantitative yield (Scheme 3).

Compound **6** has been characterised by multinuclear NMR spectroscopy and elemental analysis. The ^{1}H NMR spectrum of **6** in C_6D_6 shows the complete and regioselective conversion of alkyne **5**, with only one set of signals for the vinylic hydrogen atoms. The chemical shift of 39.6 ppm in the ^{11}B NMR spectrum is comparable to similar hydroboration products.[5d,7b,c] In analogy to previous work,[6f,g] the subsequent hydroalumination of **5** was carried out with $HAlBis_2$ [Bis = $CH(SiMe_3)_2$] under mild heating for four hours to afford PLA **7** in quantitative yield (Scheme 3). Compared to similar dialkylalanes, Bis_2AlH reacts selective towards terminal alkynes, making it suitable for the construction of this type of PLAs.[24] The ^{1}H NMR spectrum of **7** shows the expected doublets at 7.82 and 6.88 ppm with $^3J_{H,H}$ coupling constants of 20 Hz, comparable to similar hydroaluminated compounds with *trans*-arrangement of the vinylic hydrogen atoms.[6f,g,13] The chemical shift of −0.14 ppm

Table 1 Selected NMR chemical shifts [ppm] of **3**, **4** and **5** in C_6D_6 (500 MHz, 293 K)

	3	4	5
*H*1	7.28	7.42	7.34
*H*12d	3.17	3.24	3.24
$CH_2CH_2CH_3$	1.49	1.55	1.59
$CH_2CH_2CH_3$	0.84	0.88	0.85
$CH_2CH_2CH_3$	0.70	0.68	0.70

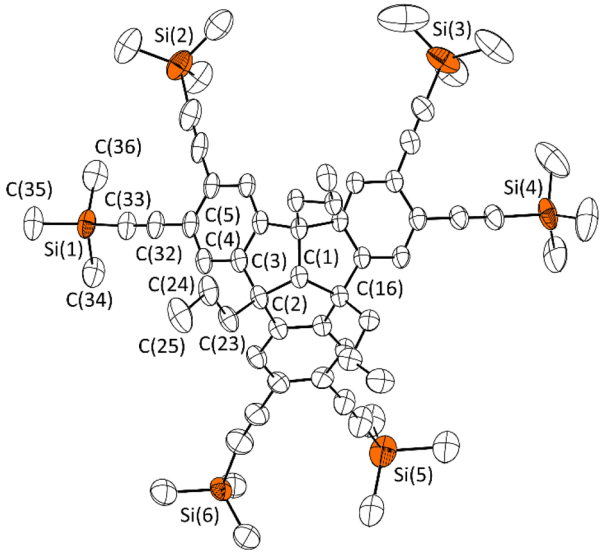

Fig. 1 Molecular structure of **4** in the crystalline state. Displacements ellipsoids are drawn at 50% probability level. Hydrogen atoms and disordered parts are omitted for clarity. Highly disordered benzene solvent molecules were treated with a solvent mask. For further details, see the ESI.† Selected bond lengths [Å] and angles [°]: C(1)–C(2) 1.569(4), C(2)–C(3) 1.513(4), C(3)–C(4) 1.396(4), C(4)–C(5) 1.397(5), C(2)–C(23) 1.536(4), C(23)–C(24) 1.515(5), C(24)–C(25) 1.522(5), C(5)–C(32) 1.433(4), C(32)–C(33) 1.209(4), Si(1)–C(33) 1.850(3), Si(1)–C(34) 1.873(4), C(1)–C(2)–C(3) 103.5(2), C(2)–C(3)–C(4) 127.6(3), C(3)–C(4)–C(5) 120.2(3), C(4)–C(5)–C(32) 120.9(3), C(5)–C(32)–C(33) 178.5(3), C(32)–C(33)–Si(1) 174.1(3), C(33)–Si(1)–C(34) 107.8(2).

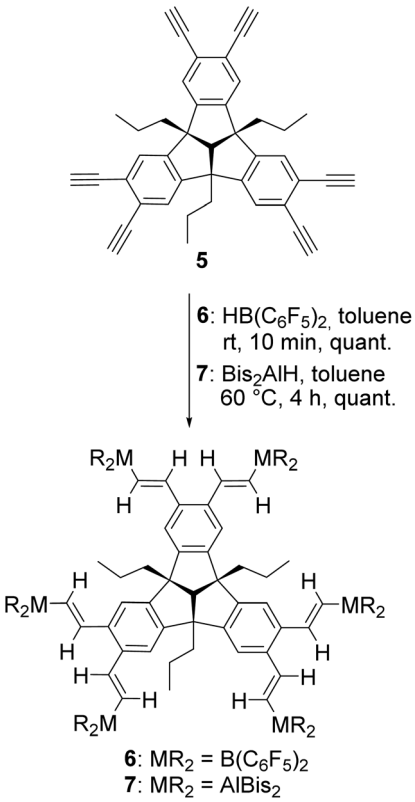

Scheme 3 Hydrometallation reaction of **5** with Piers' borane (HB$(C_6F_5)_2$) and bis(bis(trimethylsilyl)methyl)aluminium hydride (HAlBis$_2$) to give the sixfold functionalised poly-Lewis acids **6** and **7**.

for the Al–C*H* group indicates a tri-coordinated unsaturated aluminium compound. Remarkably, the Bis substituents evoke two signals at 0.40 and 0.34 ppm, due to steric hindrance of the rotation of the $SiMe_3$ groups caused by the bulky substituents. By cooling a concentrated toluene solution of **7** to −30 °C, single crystals suitable for X-ray diffraction were obtained (Fig. 2). The molecular structure of **7** confirms the formation of the kinetically favoured hydroalumination product, with the vinylic hydrogen atoms in *trans*-arrangement with planar surrounded Al atoms as suggested by the ^{1}H NMR spectrum. PLA **7** shows extended bond lengths and increased angles of the TBTQ backbone compared to compound **4** due to the flattening of the bowl shape caused by the bulky substituents. Nevertheless, the flexibility of PLA **7** may allow the complexation of certain Lewis basic guest molecules in the cavities of different sizes between the Lewis acidic aluminium functions. The Al···Al distances are 7.081(1) Å (Al(1)···Al(2)), 8.329(1) Å (Al(2)···Al(3)), and 15.674(1) Å (Al(3)···Al(6)), respectively.

Syntheses of rigid hexadentate poly-Lewis acids

A well-suited synthetic route to obtain poly-Lewis acids is the reaction of trimethyltin-substituted organic molecules with the corresponding chloro-element compound ($ClER_x$).[5c,e,f,9b,12c]

To prepare the sixfold trimethyltin-substituted TBTQ derivative **8**, the hexaethynyl compound **5** was reacted with the aminostannane Me_3SnNMe_2 in a well-established stannylation reaction (Scheme 4).[5c,25] Compound **8** was isolated in excellent yield (96%) and characterised by multinuclear NMR spectroscopy and elemental analysis. In addition, a single crystal of **8** was obtained by cooling a concentrated toluene solution to −30 °C (Fig. 3).

In terms of bond lengths and angles, the differences between derivatives **4** and **8** are minor. The bond angle Sn(3)–C(43)–C(42) of 167.5(8)° is smaller than the other Sn–C–C bond angles. As expected, the Sn···Sn distances of the adjacent Sn atoms (*e.g.* Sn(1)···Sn(2) 6.022(1) Å) are slightly smaller than the distances of the corresponding Al atoms of the hydroaluminated PLA **7**, giving an indication of the distances between the Lewis acid functions in the subsequent compounds. The sixfold tin-substituted TBTQ derivative **8** was converted with the corresponding chloro-element-compounds in tin-element exchange reactions (Scheme 4). The boron functionalised PLA **9** was obtained by conversion of compound **8** with 2-chlorobenzo[*d*][1,3,2]dioxaborole analogous to a similar reaction previously reported by our group.[5c] After washing the crude product with *n*-hexane, PLA **9** was isolated in 89% yield and characterised by multinuclear NMR spectroscopy and elemental analysis. The ^{1}H NMR spectrum shows the characteristic signal pattern for the catecholato substituents at 6.90 and 6.72 ppm. The chemical shift of 22.2 ppm in the ^{11}B NMR spectrum as well as absence of the carbon signal adjacent to

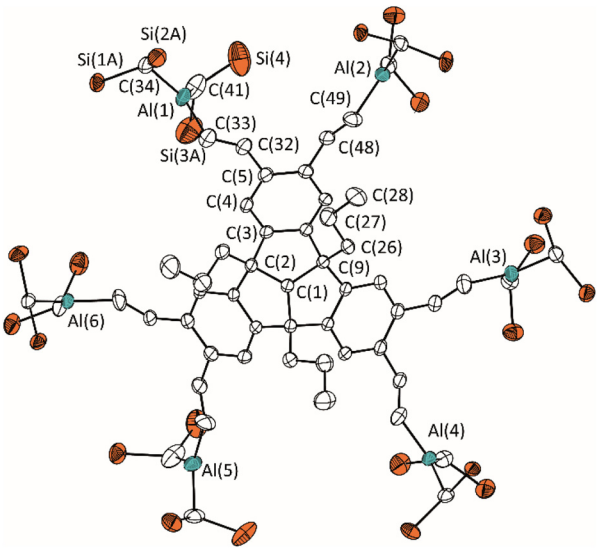

Fig. 2 Molecular structure of **7** in the crystalline state. Displacement ellipsoids are drawn at 50% probability level. Methyl C atoms and H atoms as well as disordered atoms and solvent molecules are omitted for clarity. For further details, see the ESI.† Selected bond lengths [Å] and angles [°]: C(1)–C(2) 1.560(3), C(2)–C(3) 1.649(4), C(3)–C(4) 1.426(4), C(4)–C(5) 1.509(4), C(5)–C(32) 1.518(4), C(32)–C(33) 1.322(4), Al(1)–C(33) 2.001(4), Al(1)–C(34) 1.937(3), C(1)–C(2)–C(3) 105.3(2), C(2)–C(3)–C(4) 131.2(2), C(3)–C(4)–C(5) 124.6(2), C(4)–C(5)–C(32) 124.2(2), C(5)–C(32)–C(33) 124.9(3), C(32)–C(33)–Al(1) 121.4(3), C(33)–Al(1)–C(34) 116.4(2), C(33)–Al(1)–C(41) 124.2(2), C(34)–Al(1)–C(41) 119.4(2).

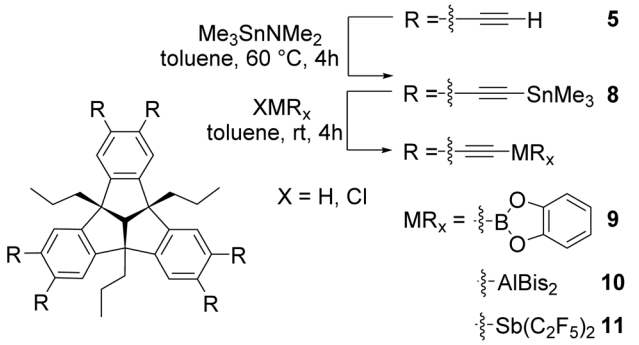

Scheme 4 Synthesis of the sixfold tin-functionalised TBTQ derivative **8** and subsequent conversion to the poly-Lewis acids **9–11** in tin-element exchange reactions.

the boron atom in the $^{13}C\{^1H\}$ NMR spectrum are consistent with related catecholato-borane compounds.[5c,e,f] Attempts to introduce Lewis acid functions by alkane elimination reactions of **5** with aluminium and gallium alkyl compounds, respectively, failed due to the lack of solubility of the formed intermediates. We expect oligomer formation by intra- and intermolecular interactions of the M–C≡C unit, which we have studied in detail in previous work.[6d] An attempt with *tert*-butyl-substituted compounds also showed no change in the solubility behaviour. Negishi *et al.* reported a selective tin–aluminium exchange with diisobutylaluminium hydride

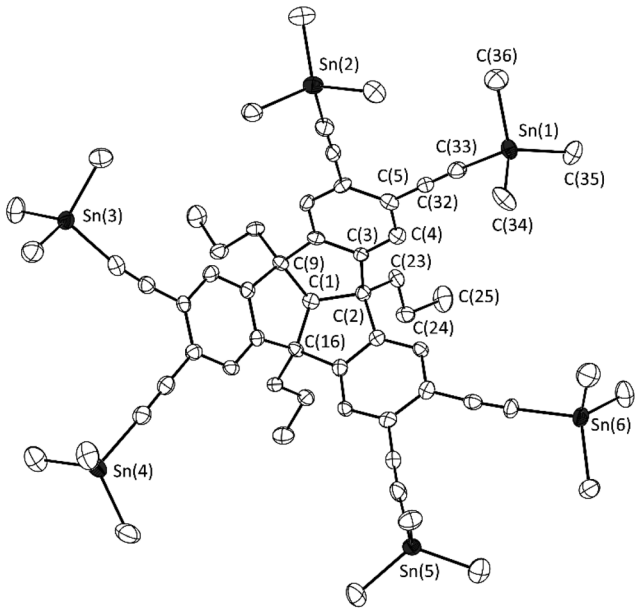

Fig. 3 Molecular structure of **8** in the crystalline state. Displacement ellipsoids are drawn at 50% probability level. Hydrogen atoms and solvent molecules are omitted for clarity. Only one of the two crystallographically independent molecules is shown. For further details, see the ESI.† Selected bond lengths [Å] and angles [°]: C(1)–C(2) 1.573(10), C(2)–C(3) 1.507(10), C(3)–C(4) 1.396(10), C(4)–C(5) 1.383(11), C(2)–C(23) 1.576(11), C(23)–C(24) 1.516(11), C(24)–C(25) 1.531(12), C(5)–C(32) 1.419(11), C(32)–C(33) 1.209(11), Sn(1)–C(33) 2.125(8), Sn(1)–C(34) 2.128(9); C(1)–C(2)–C(3) 103.9(6), C(2)–C(3)–C(4) 128.1(7), C(3)–C(4)–C(5) 121.6(7), C(4)–C(5)–C(32) 121.8(7), C(5)–C(32)–C(33) 178.6(9), C(32)–C(33)–Sn(1) 173.5(8), C(33)–Sn(1)–C(34) 103.8(3).

(DIBAL-H) and terminal tin-functionalised alkynes.[26] The reaction of stannyl-TBTQ **8** with DIBAL-H resulted in an incomplete conversion to the sixfold terminal aluminium-substituted TBTQ derivative and the formation of an insoluble solid. The analogous reaction with Bis_2AlH instead of DIBAl-H afforded PLA **10** in quantitative yield (Scheme 4). The bulky Bis substituents improve the solubility and hinder the formation of oligomeric structures between the aluminium–alkynyl functions. The aluminium functionalised PLA **10** was characterised by multinuclear NMR spectroscopy and elemental analysis. The ^1H NMR spectrum shows the expected signals for the TBTQ backbone as well as two signals for the $SiMe_3$ groups with chemical shifts of 0.48 and 0.43 ppm due to the hindered rotatability of the substituents, as already mentioned for compound **7**. Another signal at −0.24 ppm corresponds to the Al–C*H* hydrogen atoms, again characteristic for a tri-coordinated aluminium atom. The splitting of the signals of the $SiMe_3$ groups is also in agreement with the $^{13}C\{^1H\}$ and $^{29}Si\{^1H\}$ NMR spectra. By cooling of a saturated solution of **10** in *n*-hexane single crystals suitable for X-ray diffraction were obtained (Scheme 5).

The molecular structure in Fig. 4 is in agreement with the NMR spectroscopy data. It confirms the sixfold terminal functionalisation with six $AlBis_2$ groups. The bond length and angles are largely similar to that of compound **7**. The C–C–Al

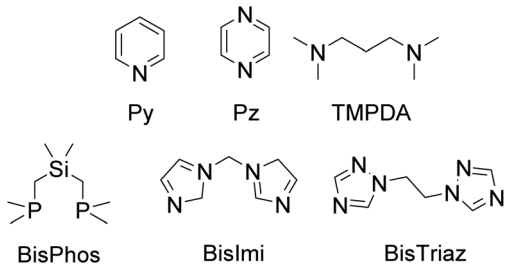

Scheme 5 Overview of the Lewis bases used in the host guest experiments. Pyridine (Py), pyrazine (Pz), *N*,*N*,*N*′,*N*′-tetramethyl-1,3-propanediamine (TMPDA) bis((dimethylphosphino)methyl)dimethylsilane (BisPhos), bis(imidazole-1-yl)methane (BisImi) and 1,2-bis(1,2,4-triazol-1-yl)ethane (BisTriaz).

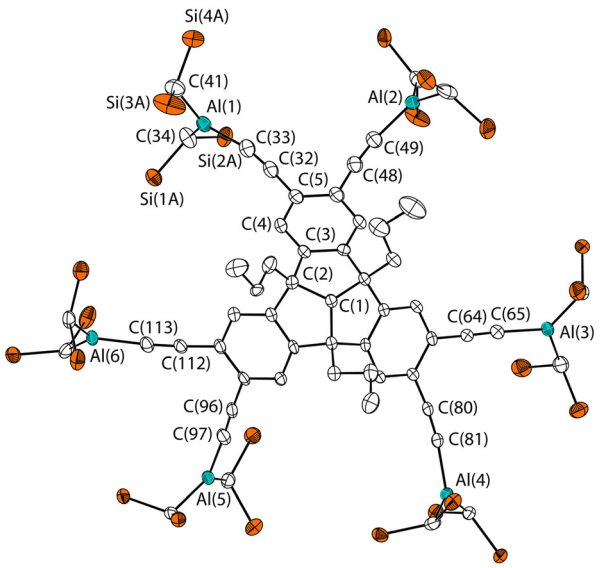

Fig. 4 Molecular structure of **10** in the crystalline state. Displacement ellipsoids are drawn at 50% probability level. Hydrogen atoms and methyl C atoms as well as disordered parts are omitted for clarity. Only one of the crystallographically independent molecules is shown. For further details, see the ESI.† Selected bond lengths [Å] and angles [°]: C(1)–C(2) 1.568(5), C(2)–C(3) 1.520(6), C(3)–C(4) 1.393(6), C(4)–C(5) 1.386(6), C(5)–C(32) 1.444(6), C(32)–C(33) 1.199(6), Al(1)–C(33) 1.903(5), Al(1)–C(34) 1.932(4), Al(1)–C(41) 1.945(5); C(1)–C(2)–C(3) 103.0(3), C(32)–C(33)–Al(1) 168.4(4), C(33)–Al(1)–C(34) 118.8(2), C(33)–Al(1)–C(41) 118.9(2), C(48)–C(49)–Al(2) 165.0(4), C(80)–C(81)–Al(4) 166.7(3), C(96)–C(97)–Al(5) 176.7(4), C(112)–C(113)–Al(6) 170.7(4).

bond angles of compound **10** differ slightly and are in the range between 165.0(4)° (C(48)–C(49)–Al(2)) and 176.7(4)° (C(96)–C(97)–Al(5)). The distances of the neighbouring Al atoms are 7.348(2) Å (Al(1)···Al(2)), 9.259(2) Å (Al(2)···Al(3)) and 16.062(2) Å (Al(3)···Al(6)) and thus slightly larger than the comparable distances of compound **7**.

Recently, we discovered the ability of antimony-based host systems with a rigid alkynyl-substituted backbone to complex Lewis basic and anionic guest molecules.[9b] Deepening the σ-hole at the antimony atom by means of pentafluoroethyl groups allows the formation of pnictogen bonds with corresponding donors such as nitrogen bases or halides. To extend this potential also to the TBTQ scaffold and generate a sixfold pnictogen-bonding donor, stannyl-TBTQ **8** was reacted with chlorobis(pentafluoroethyl)stibane in a tin–antimony exchange reaction. Removal of all volatile compounds afforded stibanyl-TBTQ derivative **11** in quantitative yield. Compound **11** was characterised by multinuclear NMR spectroscopy and elemental analysis. The ^{1}H NMR spectrum shows the expected signals for the TBTQ backbone, which are slightly shifted with respect to TBTQ derivative **8**. The absence of the $SnMe_3$ signals in samples of **11** indicates the complete conversion to **11**. In addition, the ^{1}H NMR spectrum shows the expected signal pattern for a completely and symmetrically substituted TBTQ scaffold and the ^{19}F NMR spectrum shows the two expected signals caused by the pentafluoroethyl substituents.

Host–guest experiments

For a detailed insight into the complexation behaviour of the prepared PLAs **6**, **7**, **9** and **10** towards (bidentate) Lewis-bases, several host–guest experiments with selected neutral guest molecules were performed (Scheme 5). Initial investigations with pyridine provided a benchmark for the Lewis acidity of TBTQ derivatives **6**, **7**, **9** and **10**. In all cases, formation of the corresponding 1 : 6 adduct was observed by multinuclear NMR spectroscopy (Table 2). The ^{11}B NMR spectra of PLA **6** and **9** both show high-field shifts of the signals (**6**·6Py: 4.1 ppm; **9**·6Py: 7.1 ppm). The chemical shifts are in the region of comparable tetra-coordinated borane compounds.[5e,f,12c] The ^{1}H NMR spectra are also consistent with the complexation of pyridine. Remarkably, the signals of the adduct **6**·6Py show inverted shifts for the *ortho* and *meta* hydrogen atoms of the pyridine (Table 2). For the PLAs **7** and **10**, in addition to the expected shifts of the signals, the increased hindrance to rotation of the substituents induces a further splitting of the signals of the $SiMe_3$ groups. This is also observed for the signals of the Al–C*H*Si hydrogen atoms, which experience a high-field shift (**7**·6Py −0.58 and −0.63 ppm; **10**·6Py −0.64 and −0.69 ppm), indicating the formation of a tetracoordinate aluminium atom.

In further experiments, the PLAs were complexed with bidentate bases of different size and flexibility (Scheme 5) in host guest experiments to examine a selective complexation in one of the cavities spanned between the Lewis acidic functions. Complexation of PLA **6** with rigid bidentate bases such as pyrazine (Pz) resulted in the formation of insoluble resi-

Table 2 ^{1}H NMR chemical shifts δ [ppm] in the of uncomplexed pyridine[27] and of pyridine in the corresponding adducts with the PLAs **6**, **7**, **9** and **10** in C_6D_6 (500 MHz, 293 K)

Compound	Py–H_{ortho}	Py–H_{meta}	Py–H_{para}
Pyridine	8.53	6.66	6.98
6·6Py	8.27	6.58	6.93
7·6Py	8.94	7.09	6.92
9·6Py	8.76	6.65	6.89
10·6Py	9.19	7.16	6.96

dues. Similar results were obtained for the complexation of PLA **9** with rigid nitrogen bases such as 3,3′-bipyridine as well as with more flexible bases such as TMPDA and bis(imidazole-1-yl)methane (BisImi).

We made a contrasting observation by complexation of **9** with bis((dimethylphosphino)methyl)dimethylsilane (BisPhos). Although the ^{1}H NMR spectrum shows only a slight shift of the signals of PLA **9** and the corresponding signals of the base, the singlet in the $^{31}P\{^{1}H\}$ NMR spectrum is strongly low-field shifted (−31.1 ppm, Fig. 5). In addition, the signal in the ^{11}B NMR spectrum is high-field shifted and broadened (16.7 ppm). Addition of BisPhos to PLA **7** did not result in adduct formation. The signals in the ^{1}H and $^{31}P\{^{1}H\}$ NMR spectra (Fig. 5) are slightly shifted after the addition of the base, indicating only a weak interaction between PLA **7** and BisPhos. In contrast, we observed the formation of the 3 : 1 adduct by complexation of PLA **10** with BisPhos. The signals in the ^{1}H NMR spectrum are shifted with respect to the uncomplexed PLA **10** and base. The signal of the Al–C*H* hydrogen atom is high-field shifted (−0.72 ppm) and broadened as well as the signals of the base. This is in accordance with the $^{31}P\{^{1}H\}$ NMR spectrum, which shows a broadened and shifted signal for the adduct **10**·3BisPhos (Fig. 5).

Apparently, the Lewis-acidity of the ethynyl substituted aluminium atom is enhanced compared to its vinyl substituted analogue. By concentration of a solution of **10**·3BisPhos in C_6D_6 and storing for several days, single crystals suitable for X-ray diffraction experiments were obtained (Fig. 6). The molecular structure of **10**·3BisPhos confirms the complexation of three BisPhos molecules. Despite the smaller distance between the adjacent aluminium atoms, the complexation is favoured in this Lewis acidic "pincer". The high flexibility of Lewis base (BisPhos) and the deformation of one of the alkyne-aluminium bond angles allow the selective complexation of the guest molecules. The bond angle C(112)–(C113)–Al(6) is 160.3(4)°, which is 10.4° smaller than the comparable angle in the free aluminium substituted PLA **10**. The Al–P bond lengths (*e.g.* Al(1)–P(1) 2.506(7) Å) differ only marginally from each other and are comparable to the literature data of other datively bonded aluminium–phosphorus compounds such as Me_3Al–PMe_3 (Al–P 2.53(4)).[28]

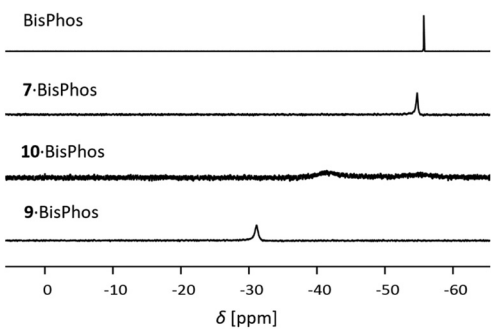

Fig. 5 Increasing low-field shift in the $^{31}P\{^{1}H\}$ NMR spectra of the BisPhos adducts of PLAs **6**, **9** and **10** (C_6D_6, 202 MHz, 293 K).

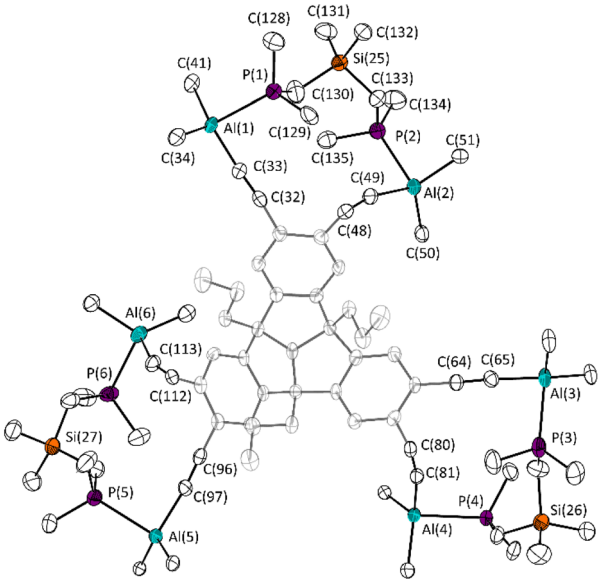

Fig. 6 Molecular structure of **10**·3BisPhos in the crystalline state. Displacement ellipsoids are drawn at 50% probability level. Hydrogen atoms, solvent molecules and minor occupied disordered parts, as well as the $SiMe_3$ groups are omitted and the TBTQ backbone is greyed out for clarity. For further details, see the ESI.† Selected bond lengths [Å] and angles [°]: C(32)–C(33) 1.210(6), Al(1)–C(33) 1.973(7), Al(1)–C(34) 1.977(8), Al(1)–C(41) 2.025(10), Al(1)–P(1) 2.506(7), P(1)–C(130) 1.866(6), C(130)–Si(25) 1.890(6); C(32)–C(33)–Al(1) 156.4(5), C(33)–Al(1)–P(1) 89.7(2), C(33)–Al(1)–C(34) 111.2(4), C(33)–Al(1)–C(41) 123.5(4), Al(1)–P(1)–C(128) 119.9(3), C(48)–C(49)–Al(2) 164.0(4). C(80)–C(81)–Al(4) 163.2(4), C(112)–C(113)–Al(6) 160.3(4).

We also observed a limited complexation behaviour of TBTQ derivative **7** also towards other bidentate, aliphatic nitrogen bases such as TMPDA, due to its lower Lewis basicity compared to pyridine and similar aromatic nitrogen bases. However, the addition of three equivalents of pyrazine to PLA **7** in C_6D_6 resulted in a colour change from yellow to red, indicating the formation of an adduct. This is in agreement with the ^{1}H NMR spectrum, which shows a high-field shift for the signals of PLA **7** with broadening of the signal for the methine hydrogen atom (Al–C*H*), and a low-field shift as well as a broadening of the pyrazine signal. The $^{29}Si\{^{1}H\}$ NMR shows only a broadened signal, in contrast to the signal splitting for the PLA adduct **7**·6Py. The addition of three equivalents of pyrazine to PLA **10** resulted in an orange colouration of the solution, although the ^{1}H NMR spectrum showed no selective formation of a 3 : 1 adduct. It is likely that the complexation resulted in the formation of oligomers by intermolecular linkage of several PLA molecules *via* pyrazine units. Addition of BisImi to **7**·6Py in THF-*d*8 solution resulted in a selective exchange of all six pyridine molecules by three equivalents of BisImi. The sharp signals in the ^{1}H NMR and $^{29}Si\{^{1}H\}$ NMR spectra, as well as the chemical shift of the methine hydrogen atoms (−0.90, −0.94), indicate that BisImi has a suitable size to fit well into the Lewis acidic "pincer" of PLA **7**. Also, the comparatively high Lewis basicity of BisImi resulted in an

adduct with less dynamic complexation, which is in agreement with the NMR spectra. We suggest that the BisImi molecules are preferentially bound in the smaller cavities (Fig. 2) due to the distance between the nitrogen atoms ($N_{BisImi}\cdots N'_{BisImi}$ = 5.807 Å).

The increased Lewis acidity of the rigid TBTQ derivative **10** compared to the hydroaluminated PLA **7** allows the complexation of further Lewis bases of lower basicity. Conversion of **10** with three equivalents of TMPDA resulted in the formation of the 3 : 1 adduct, whose ^{1}H NMR spectrum corresponds predominantly to that of **10**·3BisPhos. We assume that the TMPDA is complexed in the same cavities, due to its similar flexibility and size compared to BisPhos. Conversion of PLA **10** with the comparably sized but less flexible BisImi resulted in a mixture of two different species according to the ^{1}H NMR spectrum. Despite the limited flexibility of BisImi compared to BisPhos and TMPDA, the increased Lewis basicity results in a less dynamic Lewis acid–base interaction and thus less selective adduct formation. Complexation with the more flexible and slightly larger BisTriaz resulted in the selective formation of a 1 : 3 adduct, as indicated by the ^{1}H and ^{29}Si{^{1}H} NMR spectra, with uncertainty as to which position of the host molecule the guest is bound to. In the ^{1}H NMR spectrum, the signals of the bis(trimethylsilyl)methyl substituents are split into four ($SiMe_3$) and two (Al–C*H*) signals, respectively, similar to the ^{1}H NMR spectrum of the pyridine adduct (**10**·6Py). In addition, the signal of the methine hydrogen atom is high-field shifted and is in the region of a tetra-coordinated aluminium atom (−0.98 ppm, −1.00 ppm).

Host–guest experiments with the sixfold pnictogen-bonding donor **11** and Bu_4NI (TBAI) resulted in the conversion of compound **11** to an adduct of unknown composition. The signals in the ^{19}F NMR spectrum of this mixture are slightly shifted relative to those of pure **11**, suggesting an interaction between donor and acceptor. All attempts to obtain single crystals of the adduct were unsuccessful. Conversion of TBTQ derivative **11** with BisPhos resulted in decomposition of both **11** and the corresponding Lewis base.

Conclusions

The sixfold functionalisation of the TBTQ framework, starting from triallyl-TBTQ, provides access to a series of new TBTQ poly-Lewis acid derivatives. Hydrogenation of the allyl groups at the benzhydrylic positions increased the solubility of all subsequent compounds. We have synthesised the first hexadentate poly-Lewis acids based on the TBTQ skeleton by hydrometallation of the hexaethynyl compound **5**. Conversion of **5** in an established reaction with the corresponding aminostannane Me_3SnNMe_2 yielded the sixfold tin-functionalised TBTQ derivative **8**. Further rigid poly-Lewis acids with a TBTQ backbone were synthesised by subsequent tin-element exchange reactions. These include TBTQ backbones with six benzo[*d*][1,3,2]dioxaborole and six $Al[CH(SiMe_3)_2]_2$ (–$AlBis_2$) functions. A corresponding tin–antimony exchange yielded a novel poly-pnictogen-bonding donor with six $Sb(C_2F_5)_2$ functions, which showed first reactivities by addition of halides.

The new poly-Lewis acids were investigated in host–guest experiments with selected bidentate bases. Due to their higher Lewis acidity, the boron functionalised PLAs showed more frequent formation of polymeric structures. Bis((dimethylphosphino)methyl)dimethylsilane (BisPhos) was found to be a suitable base to form 3 : 1 adducts with the rigid PLAs **9** and **10**, where the connectivity of **10** and BisPhos was precisely elucidated by X-ray diffraction experiments. Further host–guest experiments of **10** and bidentate bases revealed a dependence between the size and flexibility of the guest molecule and the selectivity of the complexation behaviour.

Experimental section

General

4b,8b,12b-Tribromo-4b,8b,12b,12d-tetrahydrodibenzo[2,3 : 4,5]pentaleno[1,6-*ab*]indene(4,8,12-tribromotribenzotriquinacene),[16] 4b,8b,12b-triallyl-4b,8b,12b,12d-tetrahydrodibenzo[2,3 : 4,5]pentaleno[1,6-ab]indene (**1**, 4,8,12-triallyltribenzotriquinacene),[16] bis(pentafluorophenyl)borane[23] (Piers' borane) and chlorobis(pentafluoroethyl)stibane[9b] were synthesised according to literature protocols. $[(SiMe_3)_2HC]_2AlH$ (Bis_2AlH) was synthesised according to a slightly modified protocol.[29] Bis((dimethylphosphino)methyl)dimethylsilane[30] (BisPhos), bis(imidazole-1-yl)methane[31] (BisImi) and 1,2-di(1*H*-1,2,4-triazol-1-yl)ethane (BisTriaz)[32] were synthesised according to literature protocols All reagents for host–guest experiments were dried *in vacuo* or freshly distilled before use. All reactions with oxidation- or hydrolysis-sensitive substances were carried out using standard Schlenk techniques or in gloveboxes under inert nitrogen or argon atmosphere. Solvents were freshly dried and degassed (benzene, toluene and *n*-hexane, dried over Na/K alloy; *n*-pentane and Et_2O, dried over $LiAlH_4$; dichloromethane over calcium hydride and THF dried over potassium). NMR spectra were recorded on a Bruker Avance III 300 and Bruker Avance III 500 HD instrument at room temperature (293 K). The chemical shifts (δ) were measured in ppm with respect to the solvents (C_6D_6: ^{1}H NMR δ = 7.16 ppm, ^{13}C NMR δ = 128.06 ppm; $CDCl_3$: ^{1}H NMR δ = 7.26 ppm, ^{13}C NMR δ = 77.16 ppm; CD_2Cl_2: ^{1}H NMR δ = 5.32 ppm, ^{13}C NMR δ = 53.84 ppm, THF-*d*8: ^{1}H NMR δ = 1.72 ppm, 3.58 ppm, ^{13}C NMR δ = 25.31 ppm, 67.21 ppm) or referenced externally (^{11}B: $BF_3\cdot Et_2O$ ^{19}F: $CFCl_3$; ^{29}Si: $SiMe_4$; ^{31}P: 85% H_3PO_4,^{119}Sn: $SnMe_4$). Elemental analyses were performed using an HEKAtech EURO EA instrument. Assignments of the NMR-signals are based on the IUPAC guidelines and are shown in Scheme 6.

4b,8b,12b-Tri-*n*-propyltribenzotriquinacene (2)

Pd/C-catalyst (0.24 g, 2.3 mmol) was added to a solution of 4b,8b,12b-triallyltribenzotriquinancene (**1**, 2.03 g, 5.06 mmol) in MeOH (250 mL). The solution was fumigated with H_2 and stirred for 3 d. The mixture was filtered, and the filter cake washed with dichloromethane. The solvent was evaporated

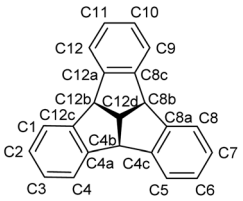

Scheme 6 Numbering scheme of tribenzotriquinacene for NMR assignments.

under reduced pressure and the colourless residue was filtered by flash column chromatography (eluent: *n*-pentane). After evaporation of the solvent and drying *in vacuo* tri-*n*-propyltribenzotriquinacene **2** was obtained as a colourless solid (2.00 g, 4.92 mmol, 98%). ^{1}H NMR (500 MHz, $CDCl_3$): δ = 7.32 (m, 6H, *H*1/*H*4/*H*5/*H*8/*H*9/*H*12), 7.15 (m, 6H, *H*2/*H*3/*H*6/*H*7/*H*10/*H*11), 3.46 (s, 1H, *H*12d), 2.06 (m, 6H, CH_2CH$_2$CH$_3$), 1.21 (m, 6H, CH$_2$CH_2CH$_3$), 0.95 (t, $^3J_{H,H}$ = 7.3 Hz, 9H, CH$_2$CH$_2$CH_3) ppm. ^{13}C{^{1}H} NMR (126 MHz, $CDCl_3$): δ = 148.9 (*C*4a/*C*4c/*C*8a/*C*8c/*C*12a/*C*12c), 127.5 (*C*2/*C*3/*C*6/*C*7/*C*10/*C*11), 123.1 (*C*1/*C*4/*C*5/*C*8/*C*9/*C*12), 67.8 (*C*12d), 63.9 (*C*4b/*C*8b/*C*12b), 44.2 (*C*H$_2$CH$_2$CH$_3$), 19.4 (*C*H$_2$CH$_2$CH$_3$), 14.9 (CH$_2$CH$_2$*C*H$_3$) ppm. Elemental analysis calcd (%) for $C_{31}H_{34}$ (406.61): C 91.57 H 8.43; found C 91.90 H 8.71.

2,3,6,7,10,11-Hexabromo-4b,8b,12b-tri-*n*-propyltribenzotriquinacene (3)

Tri-*n*-propyl-TBTQ **2** (2.80 g 6.89 mmol) was dissolved in trichloromethane (500 mL). Iron powder (0.57 g, 10 mmol) and a few crystals of iodine were added. The reaction mixture was heated to 60 °C and a solution of bromine (8.42 g, 52.7 mmol) in trichloromethane (40 mL) was added dropwise. The mixture was stirred for 16 h at 60 °C and then quenched with saturated aqueous Na_2SO_3 solution (100 mL). The mixture was extracted with dichloromethane, the organic layer was washed several times with saturated Na_2SO_3 solution and dried over $MgSO_4$. After filtration and evaporation of the solvent under reduced pressure the residue was filtered by column chromatography (eluent: *n*-pentane) to yield hexabromo-tribenzotriquinacene **3** as a pale yellow solid.^{1}H NMR (500 MHz, C_6D_6): δ = 7.28 (s, 6H, *H*1/*H*4/*H*5/*H*8/*H*9/*H*12), 3.16 (s, 1H, *H*12d), 1.49 (m, 6H, CH_2CH$_2$CH$_3$), 0.84 (m, 6H, CH$_2$CH_2CH$_3$), 0.70 (t, $^3J_{H,H}$ = 7.2 Hz, 9H, CH$_2$CH$_2$CH_3) ppm. ^{13}C{^{1}H} NMR (126 MHz, C_6D_6): δ = 148.7 (*C*4a/*C*4c/*C*8a/*C*8c/*C*12a/*C*12c), 128.4 (*C*1/*C*4/*C*5/*C*8/*C*9/*C*12) 124.8 (*C*2/*C*3/*C*6/*C*7/*C*10/*C*11), 68.4 (*C*12d), 63.06 (*C*4b/*C*8b/*C*12b), 43.0 (*C*H$_2$CH$_2$CH$_3$), 19.16 (CH$_2$*C*H$_2$CH$_3$), 14.6 (CH$_2$CH$_2$*C*H$_3$) ppm. Elemental analysis calcd (%) for $C_{31}H_{28}Br_6$ (873.73): C 42.31 H 3.21; found C 44.04 H 3.32.

2,3,6,7,10,11-Hexakis((trimethylsilyl)ethynyl)-4b,8b,12b-tri-*n*-propyltribenzotriquinacene (4)

Hexabromo-TBTQ **3**, trimethylsilylacetylene (8.00 mL, 56.2 mmol) and triphenylphosphine (1.56 g, 59.5 mmol) were suspended in triethylamine (80 mL). The suspension was degassed 3 times, $Cl_2[Pd(PPh_3)_2]$ and CuI were added and the mixture was heated to 120 °C for 3 d. The reaction was quenched with aqueous HCl-solution (3.5%, 200 mL) and extracted with dichlormethane. The organic layer was dried over $MgSO_4$, filtered and the solvent was evaporated under reduced pressure. The crude product was purified by column chromatography (eluent: *n*-pentane/dichloromethane 100 : 1). After evaporation of the solvent, hexakis((trimethylsilyl) ethynyl)-TBTQ **4** was obtained as a pale yellow solid (3.60 g, 3.8 mmol, 68%). ^{1}H NMR (500 MHz, C_6D_6): δ = 7.42 (s, 6H, *H*1/*H*4/*H*5/*H*8/*H*9/*H*12), 3.24 (s, 1H, *H*12d), 1.55 (m, 6H, CH_2CH$_2$CH$_3$), 0.88 (m, 6H, CH$_2$CH_2CH$_3$), 0.68 (t, $^3J_{H,H}$ = 7.4 Hz, 9H, CH$_2$CH$_2$CH_3) 0.32 (s, 54H, Si(CH_3)$_3$) ppm. ^{13}C{^{1}H} NMR (126 MHz, C_6D_6): δ = 148.5 (*C*4a/*C*4c/*C*8a/*C*8c/*C*12a/*C*12c), 127.8 (*C*1/*C*4/*C*5/*C*8/*C*9/*C*12), 126.5 (*C*2/*C*3/*C*6/*C*7/*C*10/*C*11) 104.6 (*C*≡C–SiMe$_3$), 98.3 (C≡*C*–SiMe$_3$) 68.5 (*C*12d), 63.3 (*C*4b/*C*8b/*C*12b), 43.2 (*C*H$_2$CH$_2$CH$_3$), 19.2 (CH$_2$*C*H$_2$CH$_3$), 14.6 (CH$_2$CH$_2$*C*H$_3$) 0.2 Si(*C*H$_3$)$_3$ ppm. ^{29}Si{^{1}H} NMR (99 MHz, C_6D_6) δ = −18.1 ppm. Elemental analysis calcd (%) for $C_{61}H_{82}Si_6$ (983.84): C 74.47 H 8.40; found C 74.34 H 8.50.

2,3,6,7,10,11-Hexaethynyl-4b,8b,12b-tri-*n*-propyltribenzotriquinacene (5)

Compound **4** (3.00 g, 5.45 mmol) was dissolved in THF (50 mL) and DMF (50 mL). Potassium fluoride (1.64 g, 28.3 mmol) was added and the reaction mixture was stirred for 3 d at rt. The solvents were evaporated under reduced pressure and the residue was dissolved in dichloromethane and water. The phases were separated and the organic layer was dried over $MgSO_4$. After filtration and evaporation of the solvent, the crude product was purified by column chromatography (eluent: *n*-pentane/ethyl acetate 20 : 1) to afford hexaethynyltribenzotriquinacene **5** as a brown solid (1.18 g, 2.14 mmol, 40%). ^{1}H NMR (500 MHz, C_6D_6): δ = 7.34 (s, 6H, *H*1/*H*4/*H*5/*H*8/*H*9/*H*12), 3.24 (s, 1H, *H*12d), 2.97 (s, 6H, C≡C*H*) 1.60 (m, 6H, CH_2CH$_2$CH$_3$), 0.89 (m, 6H, CH$_2$CH_2CH$_3$), 0.70 (t, $^3J_{H,H}$ = 7.2 Hz, 9H, CH$_2$CH$_2$CH_3) ppm. ^{13}C{^{1}H} NMR (126 MHz, C_6D_6): δ = 148.6 (*C*4a/*C*4c/*C*8a/*C*8c/*C*12a/*C*12c), 127.6 (*C*1/*C*4/*C*5/*C*8/*C*9/*C*12) 125.8 (*C*2/*C*3/*C*6/*C*7/*C*10/*C*11), 82.3 (*C*≡C–H), 81.8 (C≡*C*–H) 68.1 (*C*12d), 63.6 (*C*4b/*C*8b/*C*12b), 43.3 (*C*H$_2$CH$_2$CH$_3$), 19.2 (CH$_2$*C*H$_2$CH$_3$), 14.6 (CH$_2$CH$_2$*C*H$_3$) ppm. Elemental analysis calcd (%) for $C_{43}H_{34}$ (550.75): C 93.78 H 6.22; found C 90.99 H 6.36.

2,3,6,7,10,11-Hexakis(bis(pentafluorophenyl)boryl)vinyl-4b,8b,12b-tri-*n*-propyltribenzotriquinacene (6)

Hexaethynyl-TBTQ **5** (12.1 mg, 0.02 mmol) was dissolved in toluene (2 mL) and bis(pentafluorophenyl)borane (46.0 mg, 0.13 mmol) was added. The mixture was stirred for 10 min until the solid was completely dissolved. Evaporation of all volatile compounds yielded hexakis(bis(pentafluorophenyl) boryl)vinyl-TBTQ **6** as a yellow solid (57.2 mg, 0.02 mmol, 100%). ^{1}H NMR (500 MHz, C_6D_6): δ = 7.94 (s, 6H, *H*1/*H*4/*H*5/*H*8/*H*9/*H*12), 7.81 (d, $^3J_{H,H}$ = 17.5 Hz, 6H, (R^F)$_2$B–C*H*=CH), 7.55 (d, $^3J_{H,H}$ = 17.5 Hz, 6H, (R^F)$_2$B–CH=C*H*), 3.77 (s, 1H, *H*12d), 2.22 (m, 6H, CH_2CH$_2$CH$_3$), 1.30 (m, 6H, CH$_2$CH_2CH$_3$), 0.84 (t, $^3J_{H,H}$ = 7.2 Hz, 9H, CH$_2$CH$_2$CH_3) ppm. ^{11}B NMR

(160 MHz, C_6D_6): 39.6 (s, br) ppm. $^{13}C\{^1H\}$ NMR (126 MHz, C_6D_6): δ = 159.0 ($(R^F)_2B$–*C*H=CH), 151.6 (*C*4a/*C*4c/*C*8a/*C*8c/*C*12a/*C*12c), 149.2 (*m*-C(Ph^F)) 147.1 (*p*-C(Ph^F)), 138.8 ($(R^F)_2B$–CH=*C*H), 136.7 (*o*-C(Ph^F)), 123.9 (*C*1/*C*4/*C*5/*C*8/*C*9/*C*12), 113.5 (*C*2/*C*3/*C*6/*C*7/*C*10/*C*11), 100.4 (*C*12d), 64.5 (*C*4b/*C*8b/*C*12b), 43.9 ($CH_2CH_2CH_3$), 19.6 ($CH_2CH_2CH_3$), 14.7 ($CH_2CH_2CH_3$). ^{19}F NMR (471 MHz, C_6D_6) −129.6 (m, *o*-F(Ph^F)), 146.3 (m, *p*-F(Ph^F)), 160.9 (m, *m*-F(Ph^F)) ppm. Elemental analysis calcd (%) for $C_{115}H_{40}B_6F_{60}$ (2626.35): C 52.59 H 1.57; found C 52.59 H 1.54.

2,3,6,7,10,11-Hexakis(2-bis(bis(trimethylsilyl)methyl)aluminyl)vinyl-4b,8b,12b-tri-*n*-propyltribenzotriquinacene (7)

Compound **5** (40 mg, 0.07 mmol) was dissolved in toluene (2 mL) and Bis_2AlH (153 mg, 0.44 mmol) was added. The reaction mixture was heated to 60 °C for 4 h. All volatiles were removed and the residue was dissolved in a small amount of toluene and cooled to −30 °C. Removal of the supernatant solution and drying *in vacuo* afforded the hydroaluminated TBTQ derivative **7** as colourless crystalline solid (184 mg, 0.07 mmol, 100%). ^1H NMR (300 MHz, C_6D_6): δ = 7.87 (d, $^3J_{H,H}$ = 20.3 Hz, 6H, Bis_2Al–C*H*=CH), 7.77, (s, 6H, *H*1/*H*4/*H*5/*H*8/*H*9/*H*12), 6.93 (d, $^3J_{H,H}$ = 20.3 Hz, 6H, Bis_2Al–CH=C*H*), 3.52 (s, 1H, *H*12d), 2.17 (m, 6H, $CH_2CH_2CH_3$), 1.27 (m, 6H, $CH_2CH_2CH_3$), 0.93 (t, $^3J_{H,H}$ = 7.1 Hz, 9H, $CH_2CH_2CH_3$) 0.41/0.35 (s, 108H each signal, $AlCH(Si(CH_3)_3)_2$), −0.13 (s, 12H, Al–C*H*) ppm. $^{13}C\{^1H\}$ NMR (126 MHz, C_6D_6): δ = 149.1 (Ar–CH=*C*H), 148.9 (*C*4a/*C*4c/*C*8a/*C*8c/*C*12a/*C*12c), 141.3 (Ar–*C*H=CH), 138.9 (*C*2/*C*3/*C*6/*C*7/*C*10/*C*11), 121.0 (*C*1/*C*4/*C*5/*C*8/*C*9/*C*12), 63.3 (*C*4b/*C*8b/*C*12b), 45.1 (*C*12d), 31.6 ($CH_2CH_2CH_3$), 22.7 ($CH_2CH_2CH_3$), 14.0 ($CH_2CH_2CH_3$), 9.8 (Al–*C*H), 4.5/4.3 (AlCH–Si*Me*$_3$) ppm. $^{29}Si\{^1H\}$ (99 MHz, C_6D_6) δ = −3.3, −3.5 ppm. Elemental analysis calcd (%) for $C_{127}H_{268}Al_6Si_{24}$ (2631.47): C 57.97 H 10.27; found C 55.93 H 11.08.

2,3,6,7,10,11-Hexakis((trimethylstannyl)ethynyl)-4b,8b,12b-tri-*n*-propyltribenzotriquinacene (8)

Hexaethynyl-TBTQ **5** (200 mg 3.60 mmol) was dissolved in toluene (4 mL). Me_3SnNMe_2 (0.61 g, 2.9 mmol) was added, and the reaction mixture was heated to 60 °C for 4 h. After removing all volatile compounds hexakis((trimethylstannyl)ethynyl)-TBTQ **8** was obtained as an off-white solid (528 mg, 3.50 mmol, 96%) ^1H NMR (500 MHz, C_6D_6): δ = 7.52, (s, 6H, *H*1/*H*4/*H*5/*H*8/*H*9/*H*12), 3.27 (s, 1H, *H*12d), 1.61 (m, 6H, $CH_2CH_2CH_3$), 0.94 (m, 6H, $CH_2CH_2CH_3$), 0.66 (t, $^3J_{H,H}$ = 7.3 Hz, 9H, $CH_2CH_2CH_3$), 0.29 (s, 54H, $Sn(CH_3)_3$) ppm. $^{13}C\{^1H\}$ NMR (126 MHz, C_6D_6): δ = 148.2 (*C*4a/*C*4c/*C*8a/*C*8c/*C*12a/*C*12c), 126.9 (*C*1/*C*4/*C*5/*C*8/*C*9/*C*12), 126.6 (*C*2/*C*3/*C*6/*C*7/*C*10/*C*11), 108.4 (*C*≡CSnMe_3), 96.8 (C≡*C*SnMe_3), 68.2 (*C*12d), 63.3 (*C*4b/*C*8b/*C*12b), 43.2 ($CH_2CH_2CH_3$), 18.8 ($CH_2CH_2CH_3$), 14.2 ($CH_2CH_2CH_3$), 7.7 (Sn*Me*$_3$) ppm.$^{119}Sn\{^1H\}$ (187 MHz, C_6D_6) δ = −68.0 ppm. Elemental analysis calcd (%) for $C_{61}H_{82}Sn_6$ (1527.29): C 47.96 H 5.41; found C 46.70 H 5.58.

2,3,6,7,10,11-Hexakis((benzo[*d*][1,3,2]dioxaborol-2-yl)ethynyl)-4b,8b,12b-tri-*n*-propyltribenzotriquinacene (9)

Hexastannyl-TBTQ **8** (265 mg, 0.17 mmol) was dissolved in toluene (5 mL) and cooled to 0 °C. A solution of 2-chlorobenzo[*d*][1,3,2]dioxaborole (169 mg, 1.06 mmol) in toluene (5 mL) was added dropwise and the reaction mixture was stirred for 4 h. The solvent was evaporated under reduced pressure. The crude product was washed with *n*-hexane (2 × 2 mL), centrifuged (2000 rpm) and the supernatant solution was removed with a syringe. Drying of the residue *in vacuo* afforded **9** as a beige solid (189 mg, 0.15 mmol, 89%) ^1H NMR (300 MHz, C_6D_6): δ = 7.39, (s, 6H, *H*1/*H*4/*H*5/*H*8/*H*9/*H*12), 6.89 (m, 12H, Cat-*H*), 6.72 (m, 12H, Cat-*H*) 3.31 (s, 1H, *H*12d), 1.64 (m, 6H, $CH_2CH_2CH_3$), 0.93 (m, 6H, $CH_2CH_2CH_3$), 0.84 (t, $^3J_{H,H}$ = 6.3 Hz, 9H, $CH_2CH_2CH_3$), ppm. ^{11}B NMR (160 MHz, C_6D_6) δ = 22.4 (s, br) ppm. $^{13}C\{^1H\}$ NMR (126 MHz, C_6D_6): δ = 149.7 (*C*4a/*C*4c/*C*8a/*C*8c/*C*12a/*C*12c), 148.5 (Cat*C*O), 125.8 (*C*1/*C*4/*C*5/*C*8/*C*9/*C*12) 123.3 (Cat*C*H), 123.0 (*C*2/*C*3/*C*6/*C*7/*C*10/*C*11), 113.0 (Cat*C*H), 112.6 (*C*≡CBCat), 101.9 (*C*12d) 64.0 (*C*4b/*C*8b/*C*12b), 43.1 ($CH_2CH_2CH_3$), 19.3 ($CH_2CH_2CH_3$), 14.6 ($CH_2CH_2CH_3$) ppm. Elemental analysis calcd (%) for $C_{79}H_{46}B_6O_{12}$ (1252.09): C 75.78 H 3.70; found C 71.03 H 4.31.

2,3,6,7,10,11-Hexakis(2-bis(bis((trimethylsilyl)methyl)aluminyl)ethynyl)-4b,8b,12b-tri-*n*-propyltribenzotriquinacene (10)

Hexastannyl-TBTQ **8** (60 mg, 0.04 mmol) was dissolved in toluene (2 mL). Bis_2AlH (42 mg, 0.12 mmol) was added and the mixture was stirred at room temperature. After a few minutes both solids were dissolved, and the mixture was stirred for 4 h at room temperature. All volatile compounds were removed and compound **10** was afforded as an off-white solid (103 mg, 0.04 mmol, 100%). ^1H NMR (500 MHz, C_6D_6): δ = 7.62, (s, 6H, *H*1/*H*4/*H*5/*H*8/*H*9/*H*12), 3.28 (s, 1H, *H*12d), 1.87 (m, 6H, $CH_2CH_2CH_3$), 1.01 (m, 6H, $CH_2CH_2CH_3$), 0.81 (t, $^3J_{H,H}$ = 7.2 Hz, 9H, $CH_2CH_2CH_3$), 0.48/0.43 (s, 108H each signal, $AlCH(Si(CH_3)_3)_2$), −0.24 (s, 12H, Al–C*H*) ppm. $^{13}C\{^1H\}$ NMR (126 MHz, C_6D_6): δ = 148.5 (*C*4a/*C*4c/*C*8a/*C*8c/*C*12a/*C*12c), 125.7 (*C*2/*C*3/*C*6/*C*7/*C*10/*C*11), 112.07 (*C*≡C$AlBis_2$), 100.4 (C≡*C*$AlBis_2$) 108.1 (*C*1/*C*4/*C*5/*C*8/*C*9/*C*12), 69.1 (*C*4b/*C*8b/*C*12b), 63.5 (*C*12d), 44.5 ($CH_2CH_2CH_3$), 19.2 ($CH_2CH_2CH_3$), 14.8 ($CH_2CH_2CH_3$), 11.1 (Al–*C*H), 4.7/4.5 (AlCH–Si*Me*$_3$) ppm. $^{29}Si\{^1H\}$ (99 MHz, C_6D_6) δ = −2.8, −3.0 ppm. Elemental analysis calcd (%) for $C_{127}H_{256}Al_6Si_{24}$ (2619.37): C 58.24 H 9.85; found C 55.09 H 9.90.

2,3,6,7,10,11-Hexakis(((pentafluroethyl)stibanyl)ethynyl)-4b,8b,12b-tri-*n*-propyltribenzotriquinacene (11)

Stannane **8** (300 mg, 0.20 mmol) was dissolved in toluene (10 mL). $ClSb(C_2F_5)_2$ (632 mg, 1.30 mmol) dissolved in toluene was added and the reaction mixture was stirred for 4 h at room temperature. Removal of all volatile compounds afforded **11** as a yellow solid (540 mg, 0.20 mmol, 100%). ^1H NMR (500 MHz, C_6D_6): δ = 7.50, (s, 6H, *H*1/*H*4/*H*5/*H*8/*H*9/*H*12), 3.27 (s, 1H, *H*12d), 1.56 (m, 6H, $CH_2CH_2CH_3$), 0.85 (m, 6H, $CH_2CH_2CH_3$),

0.63 (t, $^{3}J_{H,H}$ = 7.2 Hz, 9H, $CH_2CH_2CH_3$) ppm. $^{13}C\{^{1}H\}$ NMR (126 MHz, C_6D_6): δ = 149.8 (*C*4a/*C*4c/*C*8a/*C*8c/*C*12a/*C*12c), 125.2 (*C*1/*C*4/*C*5/*C*8/*C*9/*C*12), 121.4 (CF_2) 119.2 (CF_3) 114.0 (*C*≡CSb), 113.9 (*C*2/*C*3/*C*6/*C*7/*C*10/*C*11), 85.5 (C≡*C*Sb), 67.5 (*C*12d), 64.03 (*C*4b/*C*8b/*C*12b), 42.7 ($CH_2CH_2CH_3$), 19.2 ($CH_2CH_2CH_3$), 14.4 ($CH_2CH_2CH_3$) ppm. ^{19}F (126 MHz, C_6D_6) δ = −81.6 (CF_3), −106.2 (m, CF_2), −108.7 (m, CF_2) ppm. Elemental analysis calcd (%) for $C_{61}H_{82}F_{60}Sb_6$ (2703.43): C 29.77 H 1.04; found C 31.42 H 1.09.

General procedure for the host guest experiments

15 mg of the PLA was dissolved in a NMR tube fitted with a PTFE tap in C_6D_6, THF-*d*8 or CD_2Cl_2 (0.5 mL) followed by addition of the Lewis base. After mixing, the solutions were analysed by multinuclear NMR spectroscopy. NMR data are given below.

PLA 6·6Py

^{1}H NMR (500 MHz, C_6D_6): δ = 8.27 (m, Py-H_{meta}), 8.11 (s, 6H, *H*1/*H*4/*H*5/*H*8/*H*9/*H*12), 7.29 (d, $^{3}J_{H,H}$ = 17.5 Hz, 6H, $(R^F)_2B$–C*H*═CH), 6.92 (m, Py-H_{para}), 6.77 (d, $^{3}J_{H,H}$ = 17.5 Hz, 6H, $(R^F)_2B$–CH═C*H*), 6.58 (m, Py-H_{ortho}), 3.72 (s, 1H, *H*12d), 2.32 (m, 6H, $CH_2CH_2CH_3$), 1.34 (m, 6H, $CH_2CH_2CH_3$), 0.68 (t, $^{3}J_{H,H}$ = 7.2 Hz, 9H, $CH_2CH_2CH_3$) ppm. ^{11}B NMR (160 MHz, C_6D_6): 4.1 (s, br) ppm. ^{19}F NMR (471 MHz, C_6D_6) −131.9 (m, *o*-F(Ph^F)), 157.9 (m, *p*-F(Ph^F)), 163.6 (m, *m*-F(Ph^F)) ppm.

PLA 7·6Py

^{1}H NMR (300 MHz, C_6D_6): δ = 8.94 (m, Py-H_{meta}), 8.05 (s, 6H, *H*1/*H*4/*H*5/*H*8/*H*9/*H*12), 7.82 (d, $^{3}J_{H,H}$ = 20.3 Hz, 6H, Bis_2Al–C*H*═CH), 7.21 (d, $^{3}J_{H,H}$ = 20.3 Hz, 6H, Bis_2Al–CH═C*H*), 7.06 (m, Py-H_{para}), 6.89 (m, Py-H_{ortho}), 3.67 (s, 1H, *H*12d), 2.33 (m, 6H, $CH_2CH_2CH_3$), 1.44 (m, 6H, $CH_2CH_2CH_3$), 1.03 (t, $^{3}J_{H,H}$ = 7.1 Hz, 9H, $CH_2CH_2CH_3$) 0.41/0.34/0.33/0.12 (s, 54H each signal, $AlCH(Si(CH_3)_3)_2$), −0.58/ −0.62 (s, 6H each signal, Al–C*H*) ppm. $^{29}Si\{^{1}H\}$ NMR (99 MHz, C_6D_6) δ = −1.6, −1.9, −2.0, −2.5 ppm.

PLA 9·6Py

^{1}H NMR (500 MHz, CD_2Cl_2): δ = 8.98 (m, Py-H_{meta}), 7.96 (m, Py-H_{para}), 7.62 (m, Py-H_{ortho}), 7.38, (s, 6H, *H*1/*H*4/*H*5/*H*8/*H*9/*H*12), 6.84 (m, 12H, Cat-*H*), 6.76 (m, 12H, Cat-*H*), 3.42 (s, 1H, *H*12d), 1.93 (m, 6H, $CH_2CH_2CH_3$), 1.10 (m, 6H, $CH_2CH_2CH_3$), 0.89 (t, $^{3}J_{H,H}$ = 6.3 Hz, 9H, $CH_2CH_2CH_3$), ppm. ^{11}B NMR (160 MHz, CD_2Cl_2) δ = 7.1 (s, br) ppm.

^{1}H NMR (300 MHz, CD_2Cl_2): δ = 8.76 (m, Py-H_{meta}) 7.23, (s, 6H, *H*1/*H*4/*H*5/*H*8/*H*9/*H*12), 7.00 (m, 12H, Cat-*H*), 6.89 (m, 12H, Cat-*H*), 6.82 (m, Py-H_{para}), 6.65 (m, Py-H_{ortho}), 3.22 (s, 1H, *H*12d), 1.62 (m, 6H, $CH_2CH_2CH_3$), 0.91 (m, 6H, $CH_2CH_2CH_3$), 0.69 (t, $^{3}J_{H,H}$ = 6.9 Hz, 9H, $CH_2CH_2CH_3$) ppm.

PLA 10·6Py

^{1}H NMR (500 MHz, C_6D_6): δ = 9.19 (m, Py-H_{meta}), 7.87 (s, 6H, *H*1/*H*4/*H*5/*H*8/*H*9/*H*12), 7.16 (m, Py-H_{para}), 6.96 (m, Py-H_{ortho}), 3.58 (s, 1H, *H*12d), 2.14 (m, 6H, $CH_2CH_2CH_3$), 1.27 (m, 6H, $CH_2CH_2CH_3$), 0.96 (t, $^{3}J_{H,H}$ = 7.1 Hz, 9H, $CH_2CH_2CH_3$), 0.46/0.45/0.27 (s, 216H, $AlCH(Si(CH_3)_3)_2$), −0.64/−0.69 (s, 6H each signal, Al–C*H*) ppm. $^{29}Si\{^{1}H\}$ (99 MHz, C_6D_6) δ = −1.35, −1.37, −1.89, −2.08 ppm.

PLA 7·3Pz

^{1}H NMR (300 MHz, C_6D_6): δ = 9.02 (s, br, Pz–*H*), 7.80 (d, $^{3}J_{H,H}$ = 19.9 Hz, 6H, Bis_2Al–C*H*═CH), 7.49 (s, 6H, *H*1/*H*4/*H*5/*H*8/*H*9/*H*12), 6.72 (d, $^{3}J_{H,H}$ = 19.9 Hz, 6H, Bis_2Al–CH═C*H*), 3.46 (s, 1H, *H*12d), 2.11 (m, 6H, $CH_2CH_2CH_3$), 1.21 (m, 6H, $CH_2CH_2CH_3$), 0.88 (t, $^{3}J_{H,H}$ = 7.1 Hz, 9H, $CH_2CH_2CH_3$) 0.33/0.29 (s, 108H each signal $AlCH(Si(CH_3)_3)_2$), −0.49, (s, br, 12H, Al–C*H*) ppm. $^{29}Si\{^{1}H\}$ (99 MHz, C_6D_6) δ = −2.3 (br) ppm.

PLA 7·3BisImi

^{1}H NMR (300 MHz, THF-*d*8): δ 7.71(s, 12H, BisImi-*H*), 7.62 (s, 6H, BisImi-*H*), 7.42 (s, 6H, *H*1/*H*4/*H*5/*H*8/*H*9/*H*12), 7.31 (d, $^{3}J_{H,H}$ = 20.6 Hz, 6H, Bis_2Al–C*H*═CH), 7.04 (d, $^{3}J_{H,H}$ = 20.4 Hz, 6H, Bis_2Al–CH═C*H*), 3.39 (s, 1H, *H*12d), 2.06 (m, 6H, $CH_2CH_2CH_3$), 1.17 (m, 6H, $CH_2CH_2CH_3$), 0.92 (t, $^{3}J_{H,H}$ = 6.9 Hz, 9H, $CH_2CH_2CH_3$) 0.20, 0.05, −0.03, −0.06 (s, 54H each signal, $AlCH(Si(CH_3)_3)_2$), −0.90, −0.94 (s, 6H each signal Al–C*H*) ppm. $^{29}Si\{^{1}H\}$ (99 MHz, THF-*d*8) δ = −1.74, −1.80, −2.21, −2.24 ppm.

PLA 9·3BisPhos

^{1}H NMR (500 MHz, C_6D_6): δ = 7.35, (s, 6H, *H*1/*H*4/*H*5/*H*8/*H*9/*H*12), 6.91 (m, 12H, Cat-*H*), 6.73 (m, 12H, Cat-*H*) 3.29 (s, 1H, *H*12d), 1.65 (m, 6H, $CH_2CH_2CH_3$), 0.99 (m, 6H, $CH_2CH_2CH_3$), 0.92 (m, PCH_3) 0.80 (t, $^{3}J_{H,H}$ = 6.3 Hz, 9H, $CH_2CH_2CH_3$), 0.28 ($MeSi(CH_2PMe_2)_2$), 0.23 (CH_3Si) ppm. ^{11}B NMR (160 MHz, C_6D_6) δ = 17.0 (s, br) ppm. $^{31}P\{^{1}H\}$ NMR (202 MHz, C_6D_6) δ = −31.1 ppm.

PLA 10·3BisPhos

^{1}H NMR (500 MHz, C_6D_6): δ = 7.70 (s, 6H, *H*1/*H*4/*H*5/*H*8/*H*9/*H*12), 3.41 (s, 1H, *H*12d), 1.88 (m, 6H, $CH_2CH_2CH_3$), 1.21 (m, 6H, $CH_2CH_2CH_3$), 1.12 (s, br, 18H PCH_3), 1.00 (m, br, 12H, Me_3SiCH_2), 0.90 (t, $^{3}J_{H,H}$ = 7.1 Hz, 9H, $CH_2CH_2CH_3$), 0.52, 0.46, (s, 108H each signal, $AlCH(Si(CH_3)_3)_2$), −0.71 (s, br, 12H, Al–C*H*) ppm. $^{31}P\{^{1}H\}$ NMR (202 MHz, C_6D_6) δ = 42.6 (s, br) ppm.

PLA 10·3TMPDA

^{1}H NMR (500 MHz, C_6D_6): δ = 7.66 (s, 6H, *H*1/*H*4/*H*5/*H*8/*H*9/*H*12), 3.32 (s, 1H, *H*12d), 2.53 (m, br, 18H NCH_2CH_2), 2.29 (s, br, 12H, NCH_3), 1.87 (m, 6H, $CH_2CH_2CH_3$), 1.13 (m, 6H, $CH_2CH_2CH_3$), 0.89 (t, $^{3}J_{H,H}$ = 7.1 Hz, 9H, $CH_2CH_2CH_3$), 0.57/0.46 (s, 108H each signal, $AlCH(Si(CH_3)_3)_2$), −0.93, (s, br, 12H, Al–C*H*) ppm.$^{29}Si\{^{1}H\}$ (99 MHz, C_6D_6) δ = −1.36, −1.62.

PLA 10·3BisTriaz

^{1}H NMR (500 MHz, THF-*d*8): δ = 8.72 (s, 12H, triazole-*H*), 7.66 (s, 6H, *H*1/*H*4/*H*5/*H*8/*H*9/*H*12), 4.90 (NCH_2) 3.32 (s, 1H, *H*12d), 2.53 (m, br, 6H NCH_2CH_2), 2.29 (s, br, 12H, NCH_3), 1.93 (m, 6H, $CH_2CH_2CH_3$), 1.04 (m, 6H, $CH_2CH_2CH_3$), 0.90 (t, $^{3}J_{H,H}$ = 7.0 Hz, 9H, $CH_2CH_2CH_3$), 0.36, 0.21, −0.05 (s, 216H, AlCH(Si

$(CH_3)_3)_2$), −0.98, −1.00 (s, 6H each signal, Al–C*H*) ppm. ^{29}Si $\{^1$H$\}$ (99 MHz, THF-*d*8) δ = −1.23, −1.16, −1.98, −2.04 ppm.

PLA 11·3TBAI

^{1}H NMR (500 MHz, C_6D_6): δ = 7.50, (s, 6H, *H*1/*H*4/*H*5/*H*8/*H*9/*H*12), 3.27 (s, 1H, *H*12d), 2.29 (m, 24H, NCH_2) 1.55 (m, 6H, $CH_2CH_2CH_3$), 1.03 (m, 24H, NCH_2CH_2) 0.90 (m, 24H, $NCH_2CH_2CH_2$), 0.84 (m, 6H, $CH_2CH_2CH_3$), 0.80 (t, 36H, $NCH_2CH_2CH_2CH_3$) 0.65 (t, $^3J_{H,H}$ = 7.2 Hz, 9H, $CH_2CH_2CH_3$) ppm. ^{19}F (126 MHz, C_6D_6) δ = −81.5 (CF_3), −106.3 (m, CF_2), −108.8 (m, CF_2) ppm.

Conflicts of interest

There are no conflicts to declare.

Acknowledgements

The authors thank Dr Andreas Mix for recording NMR spectra and Barbara Teichner for measuring CHN analyses. We gratefully acknowledge financial support from the Deutsche Forschungsgemeinschaft (DFG, German Research Foundation, grant number MI477/39-1, project no. 424957011).

References

1 (*a*) C. J. Pedersen, *J. Am. Chem. Soc.*, 1967, **89**, 7017; (*b*) B. Dietrich, J. M. Lehn and J. P. Sauvage, *Tetrahedron Lett.*, 1969, **10**, 2885.

2 (*a*) J. D. Beckwith, M. Tschinkl, A. Picot, M. Tsunoda, R. Bachman and F. P. Gabbaï, *Organometallics*, 2001, **20**, 3169; (*b*) H. Schmidbaur, H.-J. Öller, D. L. Wilkinson, B. Huber and G. Müller, *Chem. Ber.*, 1989, **122**, 31.

3 (*a*) K. Tamao, T. Hayashi, Y. Ito and M. Shiro, *J. Am. Chem. Soc.*, 1990, **14**, 5679; (*b*) J. Horstmann, M. Niemann, K. Berthold, A. Mix, B. Neumann, H.-G. Stammler and N. W. Mitzel, *Dalton Trans.*, 2017, **46**, 1898; (*c*) D. Brondani, F. H. Carré, R. J. P. Corriu, J. J. E. Moreau and M. Wong Chi Man, *Angew. Chem.*, 1996, **108**, 349.

4 (*a*) M. Schulte, G. Gabriele, M. Schürmann, K. Jurkschat, A. Duthie and D. Dakternieks, *Organometallics*, 2003, **22**, 328; (*b*) R. Altmann, K. Jurkschat, M. Schürmann, D. Dakternieks and A. Duthie, *Organometallics*, 1998, **17**, 5858; (*c*) M. Newcomb and M. T. Blanda, *Tetrahedron Lett.*, 1988, **34**, 4261.

5 (*a*) H. E. Katz, *J. Org. Chem.*, 1985, **25**, 2057; (*b*) D. F. Shriver and M. J. Biallas, *J. Am. Chem. Soc.*, 1967, **89**, 1078; (*c*) P. Niermeier, S. Blomeyer, Y. K. J. Bejaoui, J. L. Beckmann, B. Neumann, H.-G. Stammler and N. W. Mitzel, *Angew. Chem., Int. Ed.*, 2019, **58**, 1965, (*Angew. Chem.*, 2019, **131**, 1985); (*d*) J.-H. Lamm, J. Horstmann, J. H. Nissen, J.-H. Weddeling, B. Neumann, H.-G. Stammler and N. W. Mitzel, *Eur. J. Inorg. Chem.*, 2014, 4294; (*e*) F. Schäfer, J.-H. Lamm, B. Neumann, H.-G. Stammler and N. W. Mitzel, *Eur. J. Inorg. Chem.*, 2021, 3265; (*f*) F. Schäfer, B. Neumann, H.-G. Stammler and N. W. Mitzel, *Eur. J. Inorg. Chem.*, 2021, 3083; (*g*) L. Schweighauser, I. Bodoky, S. Kessler, D. Häussinger and H. Wegner, *Synthesis*, 2012, **44**, 2195.

6 (*a*) O. Saied, M. Simard and J. D. Wuest, *Organometallics*, 1996, **15**, 2345; (*b*) W. Uhl, D. Heller, M. Rohling and J. Kösters, *Inorg. Chim. Acta*, 2011, **374**, 359; (*c*) W. Uhl, F. Hannemann, W. Saak and R. Wartchow, *Eur. J. Inorg. Chem.*, 1998, 921; (*d*) J. Chmiel, B. Neumann, H.-G. Stammler and N. W. Mitzel, *Chem. – Eur. J.*, 2010, **16**, 11906; (*e*) W. Uhl, A. Hepp, H. Westenberg, S. Zemke, E.-U. Würthwein and J. Hellmann, *Organometallics*, 2010, **29**, 1406; (*f*) N. Aders, P. C. Trapp, J.-H. Lamm, J. L. Beckmann, B. Neumann, H.-G. Stammler and N. W. Mitzel, *Organometallics*, 2022, **41**, 3600; (*g*) N. Aders, J.-H. Lamm, J. L. Beckmann, B. Neumann, H.-G. Stammler and N. W. Mitzel, *Dalton Trans.*, 2022, **51**, 12943.

7 (*a*) P. Jutzi, J. Izundu, H. Sielemann, B. Neumann and H.-G. Stammler, *Organometallics*, 2009, **28**, 2619; (*b*) E. Weisheim, C. G. Reuter, P. Heinrichs, Y. V. Vishnevskiy, A. Mix, B. Neumann, H.-G. Stammler and N. W. Mitzel, *Chem. – Eur. J.*, 2015, **21**, 12436; (*c*) E. Weisheim, L. Bücker, B. Neumann, H.-G. Stammler and N. W. Mitzel, *Dalton Trans.*, 2016, **45**, 198; (*d*) J. Horstmann, M. Hyseni, A. Mix, B. Neumann, H.-G. Stammler and N. W. Mitzel, *Angew. Chem., Int. Ed.*, 2017, **56**, 6344; (*e*) W. Uhl, M. Claesener, D. Kovert, A. Hepp, E.-U. Würthwein and N. Ghavtadze, *Organometallics*, 2011, **30**, 3075; (*f*) W. Uhl and M. Claesener, *Inorg. Chem.*, 2008, **47**, 729; (*g*) W. Uhl and M. Claesener, *Inorg. Chem.*, 2008, **47**, 4463; (*h*) J. Tomaschautzky, B. Neumann, H.-G. Stammler, A. Mix and N. W. Mitzel, *Dalton Trans.*, 2017, **46**, 1645; (*i*) W. Uhl, F. Breher, S. Haddadpour and F. Rogel, *Organometallics*, 2005, **24**, 2210.

8 F. P. Gabbaï, A. Schier, J. Riede and D. Schichl, *Organometallics*, 1996, **15**, 4119.

9 (*a*) C. R. Wade and F. P. Gabbaï, *Z. Naturforsch., B: J. Chem. Sci.*, 2014, **69**, 1199; (*b*) J. L. Beckmann, J. Krieft, Y. V. Vishnevskiy, B. Neumann, H.-G. Stammler and N. W. Mitzel, *Angew. Chem., Int. Ed.*, 2023, **62**, e202310439; C.-H. Chen and F. P. Gabbaï, *Dalton Trans.*, 2018, **47**, 12075; (*c*) C.-H. Chen and F. P. Gabbaï, *Angew. Chem.*, 2017, **129**, 1825; (*d*) M. Hirai and F. P. Gabbaï, *Angew. Chem.*, 2015, **127**, 1221.

10 (*a*) P. D. Beer and P. A. Gale, *Angew. Chem., Int. Ed.*, 2001, **40**, 486; (*b*) A. S. Wendji, C. Dietz, S. Kühn, M. Lutter, D. Schollmeyer, W. Hiller and K. Jurkschat, *Chem. – Eur. J.*, 2016, **22**, 404; (*c*) M. Melaïmi, S. Solé, C.-W. Chiu, H. Wang and F. P. Gabbaï, *Inorg. Chem.*, 2006, **45**, 8136.

11 (*a*) T. Ooi, M. Takahashi and K. Maruoka, *J. Am. Chem. Soc.*, 1996, **118**, 11307; (*b*) M. Mager, S. Becke, H. Windisch and U. Denninger, *Angew. Chem., Int. Ed.*, 2001, **40**, 1898.

12 (*a*) J.-H. Lamm, P. Niermeier, A. Mix, J. Chmiel, B. Neumann, H.-G. Stammler and N. W. Mitzel, *Angew.*

Chem., Int. Ed., 2014, **53**, 7938; (*b*) F. Schäfer, A. Mix, N. Cati, J.-H. Lamm, B. Neumann, H.-G. Stammler and N. W. Mitzel, *Dalton Trans.*, 2022, **51**, 7164; (*c*) J. Rudlof, T. Glodde, A. Mix, B. Neumann, H.-G. Stammler and N. W. Mitzel, *Eur. J. Inorg. Chem.*, 2022, e202100842.

13 (*a*) W. Uhl, M. Claesener, S. Haddadpour, B. Jasper and A. Hepp, *Dalton Trans.*, 2007, 417; (*b*) W. Uhl, H. R. Bock, M. Claesener, M. Layh, I. Tiesmeyer and E.-U. Würthwein, *Chem. – Eur. J.*, 2008, **14**, 11557.

14 (*a*) J. D. Hoefelmeyer, D. L. Brode and F. P. Gabbaï, *Organometallics*, 2001, **20**, 5653; (*b*) M. Melaimi and F. P. Gabbaï, *Z. Anorg. Allg. Chem.*, 2012, **638**, 1667.

15 D. Kuck, *Angew. Chem., Int. Ed. Engl.*, 1984, **23**, 508.

16 D. Kuck, A. Schuster, R. A. Krause, J. Tellenbröker, C. P. Exner, M. Penk, H. Bögge and A. Müller, *Tetrahedron*, 2001, 3587.

17 G. Markopoulos, L. Henneicke, J. Shen, Y. Okamoto, P. G. Jones and H. Hopf, *Angew. Chem., Int. Ed.*, 2012, **51**, 12884.

18 T. Wang, Y.-F. Zhang, Q.-Q. Hou, W.-R. Xu, X.-P. Cao, H.-F. Chow and D. Kuck, *J. Org. Chem.*, 2013, **78**, 1062.

19 (*a*) W.-R. Xu, G.-J. Xia, H.-F. Chow, X.-P. Cao and D. Kuck, *Chem. – Eur. J.*, 2015, **21**, 12011; (*b*) J. Strübe, B. Neumann, H.-G. Stammler and D. Kuck, *Chem. – Eur. J.*, 2009, **15**, 2256; (*c*) S. Klotzbach, T. Scherpf and F. Beuerle, *Chem. Commun.*, 2014, **50**, 12454; (*d*) Z. Jiang, Z. Wu, J. Wang, B. Chen, M. Wang, W. Liu, W. Lv, R. Miao, H. Zhao, D. Liu, S. Chen, M. Chen and P. Wang, *Nano Res.*, 2023, **16**, 9584.

20 (*a*) B. Bredenkötter, S. Henne and D. Volkmer, *Chem. – Eur. J.*, 2007, **13**, 9931; (*b*) B. Bredenkötter, M. Grzywa, M. Alaghemandi, R. Schmid, W. Herrebout, P. Bultinck and D. Volkmer, *Chem. – Eur. J.*, 2014, **20**, 9100; (*c*) S. Henne, B. Bredenkötter, A. A. Dehghan Baghi, R. Schmid and D. Volkmer, *Dalton Trans.*, 2012, **41**, 5995; (*d*) L. Zhou, T.-X. Zhang, B.-R. Li, X.-P. Cao and D. Kuck, *J. Org. Chem.*, 2007, **72**, 6382.

21 J. Tomaschautzky, B. Neumann, H.-G. Stammler and N. W. Mitzel, *Dalton Trans.*, 2017, **46**, 1112.

22 D. Kuck, T. Lindenthal and A. Schuster, *Chem. Ber.*, 1992, **125**, 1449.

23 D. J. Parks, R. E. v. H. Spence and W. E. Piers, *Angew. Chem., Int. Ed. Engl.*, 1995, **34**, 809.

24 W. Uhl, E. Er, A. Hepp, J. Kösters and J. Gruneberg, *Organometallics*, 2008, **27**, 3346.

25 (*a*) B. Wrackmeyer, G. Kehr and J. Süß, *Chem. Ber.*, 1993, **226**, 2221; (*b*) J.-H. Lamm, J. Glatthor, J.-H. Weddeling, A. Mix, J. Chmiel, B. Neumann, H.-G. Stammler and N. W. Mitzel, *Org. Biomol. Chem.*, 2014, **12**, 7355.

26 E. Negishi, *Organometallics in Organic Synthesis*, Wiley-Interscience, New York, 1980.

27 G. R. Fulmer, A. J. M. Miller, N. H. Sherden, H. E. Gottlieb, A. Nudelman, B. M. Stoltz, J. E. Bercaw and K. I. Goldberg, *Organometallics*, 2010, **29**, 2176.

28 A. Almenningen, L. Fernholt, A. Haaland and K. Weidlein, *J. Organomet. Chem.*, 1978, **145**, 109.

29 W. Uhl, L. Cuypers, R. Graupner, J. Molter, A. Vester and B. Neumüller, *Z. Anorg. Allg. Chem.*, 2001, **627**, 607.

30 H. H. Karsch and A. Appelt, *Z. Naturforsch., B: Anorg. Chem., Org. Chem.*, 1983, **11**, 1399.

31 E. Diez-Barra, A. Sanchez-Migallon and A. Tejeda, *Heterocycles*, 1970, **34**, 1365.

32 V. N. Kizhnyaev, E. A. Krakhotkina, T. L. Petrova, M. V. Kasantseva, F. A. Pokatinov and O. N. Verkhozina, *Polym. Sci., Ser. B*, 2010, **53**, 144.